

RESEARCH

Open Access



Predictive value of metabolic parameters and apparent diffusion coefficient derived from ^{18}F -FDG PET/MR in patients with non-small cell lung cancer

Han Jiang^{1†}, Ziqiang Li^{2†}, Nan Meng^{1†}, Yu Luo³, Pengyang Feng⁴, Fangfang Fu¹, Yang Yang⁵, Jianmin Yuan⁶, Zhe Wang⁶ and Meiyun Wang^{1*}

Abstract

Background Multiple models intravoxel incoherent motion (IVIM) based ^{18}F -fluorodeoxyglucose positron emission tomography-magnetic resonance (^{18}F -FDG PET/MR) could reflect the microscopic information of the tumor from multiple perspectives. However, its value in the prognostic assessment of non-small cell lung cancer (NSCLC) still needs to be further explored.

Objective To compare the value of ^{18}F -FDG PET/MR metabolic parameters and diffusion parameters in the prognostic assessment of patients with NSCLC.

Material and methods Chest PET and IVIM scans were performed on 61 NSCLC patients using PET/MR. The maximum standard uptake value (SUV_{max}), metabolic tumor volume (MTV), total lesion glycolysis (TLG), diffusion coefficient (D), perfusion fraction (f), pseudo diffusion coefficient (D^*) and apparent diffusion coefficient (ADC) were calculated. The impact of SUV_{max} , MTV, TLG, D , f , D^* and ADC on survival was measured in terms of the hazard ratio (HR) effect size. Overall survival time (OS) and progression-free survival time (PFS) were evaluated with the Kaplan–Meier and Cox proportional hazard models. Log-rank test was used to analyze the differences in parameters between groups.

Results 61 NSCLC patients had an overall median OS of 18 months (14.75, 22.85) and a median PFS of 17 months (12.00, 21.75). Univariate analysis showed that pathological subtype, TNM stage, surgery, SUV_{max} , MTV, TLG, D , D^* and ADC were both influential factors for OS and PFS in NSCLC patients. Multifactorial analysis showed that MTV, D^* and ADC were independent predicting factors for OS and PFS in NSCLC patients.

Conclusion MTV, D^* and ADC are independent predicting factors affecting OS and PFS in NSCLC patients. ^{18}F -FDG PET/MR-derived metabolic parameters and diffusion parameters have clinical value for prognostic assessment of NSCLC patients.

[†]Han Jiang, Ziqiang Li and Nan Meng contributed equally to this work and should be considered co-first authors.

*Correspondence:

Meiyun Wang
mywang@zzu.edu.cn

Full list of author information is available at the end of the article



Keywords Non-small cell lung cancer, Metabolic parameters, Diffusion parameters, Positron emission computed tomography, Magnetic resonance imaging

Introduction

Lung cancer is one of the most common cancers worldwide and the leading cause of cancer deaths in both developed and developing countries [1]. About 80% of the lung cancer patients are diagnosed with non-small cell lung cancer (NSCLC), and their 5-year survival rate is only 18% [1, 2]. Recent medical advances have stimulated a huge increase in overall cancer survival, but this improvement has not been ideal for lung cancer because most NSCLC has a relatively poor prognosis. Studies have shown that early assessment of prognostic factors in NSCLC patients is of great significance in determining and adjusting treatment plans, improving patient outcomes and enhancing patient quality of life [3].

Positron emission tomography-computed tomography (PET/CT) was often used to evaluate lung cancer because it was noninvasive and could provide both metabolic and morphological information about the lesion at the same time [4]. Maximum standard uptake value (SUV_{max}) represents the highest metabolic value in the lesions, and some studies found that SUV_{max} can predict the prognosis of NSCLC [5, 6]. This may be because tumors with higher pathological grade and higher stage are more heterogeneous, and cell multiplication is usually more rapid and therefore their glucose uptake is higher. Metabolic tumor volume (MTV) and total lesion glycolysis (TLG) can integrate the volume of the lesion with the metabolism, which could reflect the overall metabolism of the tumor more sufficient.

With the introduction of the concept of molecular imaging, molecular imaging techniques represented by PET magnetic resonance (PET/MR) have shown their unique advantages in displaying characteristic lesions at the tissue, reflecting changes at the molecular level in the living organism in cellular and subcellular levels, and evaluating the features of the target area qualitatively and quantitatively. In contrast to CT, PET/MR has no radiation and it can provide multiple functional parameters along with morphological and metabolic information about the focus. Meanwhile application of quantitative and semi-quantitative indicators to predict early tumor response to therapy has received most attention [7–9]. Diffusion-weighted imaging (DWI) can reflect the microstructure of tissues by obtaining motion information of water molecules. The apparent diffusion coefficient (ADC) is a quantitative indicator of the degree of diffusion limitation in DWI response. ADC values inversely correlate with cellularity, it can reflect the diffusion of water molecules in biological tissues and is usually

obviously lower in malignant tumors than normal tissues and benign lesions. Its value in distinguishing benign and malignant lesions in the lung and mediastinum is well documented, however, few articles have used it to evaluate the prognosis of lung cancer [10, 11].

The MRI technique known as Intravoxel incoherent motion (IVIM) was initially introduced by Le Bihan et al. [12]. They realized the separation of tissue water molecule diffusion from blood vessel water molecule diffusion, making up for the shortage of DWI. The most important advantage of IVIM is that, as a non-contrast perfusion imaging method, it can be used in some patients with contrast contraindications. The measurement parameters are as follows: (1) the diffusion coefficient (D), which reflects the diffusion of water molecules in interstitial tissues; (2) the perfusion fraction (f), which reflects the proportion of blood perfusion to total diffusion; and (3) the pseudo diffusion coefficient (D^*), is a false diffusion caused by blood microcirculation and belongs to rapid diffusion [13]. IVIM has already been applied to study a number of diseases, including breast cancer [14], cervical cancer [15], and prostatic cancer [16]. In this study, ^{18}F -fluorodeoxyglucose (^{18}F -FDG) PET/MR was performed to assess the prognostic value of SUV_{max} , MTV, TLG and diffusion parameter D , f , D^* and ADC in patients with NSCLC. As far as we know, these parameters are rarely used in the study of lung cancer prognosis, so our study is of great significance.

Patients and methods

Case selection and general information

This study was approved by the Ethics Committee of Henan Provincial People's hospital (2021 Lungren Trial No. 148) and each patient's written informed consent was obtained. From July 2020 to October 2021, a total of 135 patients with pulmonary lumps or nodules diagnosed by chest CT underwent chest PET/MRI. Two radiologists (N M and FF F with 10 and 15 years of experience in imaging diagnosis, respectively), blinded to the clinical and pathological information of patients, interpreted MR and PET images. The inclusion criteria were as follows: 1. Diagnosis of NSCLC confirmed by cytology or histopathology; 2. The lesions were not treated with invasive treatment, radiotherapy or chemotherapy before PET/MRI examination; 3. Clinical data of patients were complete and follow-up information could be provided. The following patients were excluded: 1. Combination of severe heart,

liver, kidney and hematopoietic diseases, severe lung dysfunction and other malignancies ($n=18$); 2. Solid lesion component cross-sectional diameter <10 mm ($n=14$); 3. No histopathological results ($n=22$); 4. Poor image quality or incomplete image sequences ($n=20$). Finally, a total of 61 patients (29 males and 32 females, age range 40–81 years) were included in this study. Analyses covered age, sex, smoking status, subtype, stage, lesion diameter, and related parameters.

Imaging protocol

All patients underwent chest scanning with an integrated 3.0 T PET/MR (uPMR790, United Imaging Medical, Shanghai, China) and a 12-channel body coil. Fasting blood glucose level were <8.0 mmol/L after at least 6 h of fasting before the examination (diabetic patients should take oral hypoglycemic drugs as prescribed to ensure fasting blood glucose <8.0 mmol/L). ^{18}F -FDG is produced by FracerLab FX-FDG (GE Minirac) with a purity of over 95% and a pH value between 4.5 and 8.5. After intravenous injection of the tracer with a dose of 0.11 mCi/kg and resting for 1 h, the patient underwent a PET scan in a supine position, connected to a breathing belt to monitor breathing, with a scanning range from the apex of the lung to the angle of the diaphragm. The Dixon MRI sequence was used in PET scanning to attenuate gamma rays, and the ordered subset maximum expected (OSME) iterative method was used for image reconstruction. Upload the data to the workstation for post-processing. Simultaneously with PET scan (27 min), axial MR based magnetic resonance attenuation correction (MRAC), T2 weighted imaging (T2WI), T1 weighted imaging (T1WI), IVIM, and DWI were performed sequentially [17]. The summary of MRI acquisition parameters is shown in Table 1.

Imaging processing

All PET/MR images were imported into a United Imaging Healthcare (UIH) workstation (uWS-MR: R005) for aftertreatment and measurement. Two radiologists (H J and ZQ L with more than 5 years of experience in imaging diagnosis), blinded to the clinical and pathological information of patients, manually delineated the regions of interest (ROIs) to allow measurement of DWI and IVIM parameters. When the patient had multiple lesions, we selected the primary lesion as the target lesion and measured its related parameters. When delineating the ROIs, the observers were required to avoid blood vessels, trachea, necrosis and bleeding to ensure selection of the solid region with uniform component [17]. The average value measured by two observers was used for statistical analysis. If necessary, solve discrepancies with the help of a third radiologist. Lesions were found on the IVIM pseudo-color map, and ROI was mapped to measure D , f , and D^* values. SUV_{max} and MTV were automatically calculated by the software, which automatically covers the whole lesion. SUV_{max} is the highest SUV value of the lesion, and a 40% SUV_{max} was applied as a threshold to quantitate the MTV. TLG is the product of MTV and mean standardized uptake value (SUV_{mean}) of the area of interest.

The parameter values of DWI and IVIM were calculated using the following equation, where b symbols the diffusion sensitivity, and ADC was computed using two b values ($0, 1000$ s/mm²) fitted to the model. $S(b)$ is the signal strength for different b values, S_0 is the signal strength at $b=0$ s/mm², f is the perfusion fraction, D is the diffusion coefficient representing actually molecular diffusion, and D^* is the pseudo-diffusion coefficient meaning separate microcirculation [18].

ADC calculation formula [19]:

Table 1 Imaging protocol parameters

Parameters	MRAC	T2WI	T1WI	DWI	IVIM
TR (msec)	4.92	3315	4.24	1620	1620
TE (msec)	2.24	87.8	1.13	69.8	69.6
FOV (mm ²)	500×350	500×350	500×350	500×350	500×350
Matrix	192×192	320×70	320×70	128×100	128×100
Slice thickness (mm)	2	5	6	5	5
Scanning time	2min4s	2min26s	14 s	40 s	3min38s
b-values (s/mm ²)	/	/	/	0, 1000	0, 25, 50, 100, 150, 200, 400, 600, 800 and 1000
Breath control	Free	Navigation	Holding	Free	Free
Orientation	Axial	Axial	Axial	Axial	Axial

MRAC MR-base attenuation correction, T2WI/T2-weighted imaging, T1WI/T1-weighted imaging, DWI Diffusion weighted imaging, IVIM Intravoxel incoherent motion, TR/TE Repetition time/echo time, FOV Field of view

$$\exp(-bADC) = \frac{S(b)}{S_0} \tag{1}$$

IVIM calculation formula:

$$S(b)/S_0 = (1 - f) \times \exp(-bD) + f \times \exp[-b \times (D^* + D)] \tag{2}$$

Treatment and follow-up

Of the 61 patients, 32 were treated surgically and 29 were treated non-surgically. Two radiologists (Y L and PY F with 3 years of experience in imaging diagnosis), blinded to the clinical and imaging information of patients, collected the follow-up data. The starting time of follow-up was the day of pathological diagnosis (or the day of surgery), and patients were followed up by case retrieval or by telephone until September 30, 2022. All patients were not missed, and the follow-up rate was 100%. Overall survival (OS) was defined as the time from pathological diagnosis to death or the end of follow-up [20]. Progression-free survival (PFS) was defined as the time from pathological diagnosis to the first detection of tumor recurrence, progression, death, or the end of follow-up.

Statistical analysis

Statistical analysis utilized SPSS 20.0, with SUV_{max}, MTV, TLG, D, f, D*, and ADC categorized as rank information data, while other count data were expressed as percentages. Interobserver reliability between two radiologists was assessed using the intragroup correlation coefficient (ICC), where ICC ≥ 0.75 indicated excellent reliability, 0.60 ≤ ICC < 0.75 indicated good reliability, ICC < 0.40 indicated poor reliability [21]. Survival curves were generated using the Kaplan–Meier method, and group differences were assessed using the Log-rank test. Cox regression analysis was employed for single-factor and multi-factor survival analysis. A significance level of P < 0.05 was applied to all statistical analyses.

Results

Consistency analysis

The parameters measured by the two researchers were in excellent agreement. The ICC values of D, f, D*, ADC were 0.847, 0.956, 0.966, 0.900 respectively. The average value of the two reader parameters is used for subsequent analyses. The values include SUV_{max}, MTV and TLG were measured by workstation software automatically, and there was no need for a consistency check.

Images and survival

Among the 61 patients, there were 29 males and 32 females with age (62.85 ± 9.63). Moreover, there are 38 patients with disease progression or death, and 23

without progression. Patients had an overall median OS of 18 months (14.75, 22.85) and a median PFS of 17 months (12.00, 21.75). The clinicopathological characteristics are shown in Table 2.

Univariate and multifactorial analysis of prognostic impact

The results of univariate analysis showed that SUV_{max}, MTV, TLG, D, D* and ADC were all influential factors for OS and PFS in NSCLC patients among PET/MR-derived metabolic and diffusion parameters (P < 0.05). Among clinical factors, pathological subtype, TNM stage (TNM classification, 8th edition, 2014) and surgery were influential factors for OS and PFS in NSCLC patients (P < 0.05). Factors that were statistically significant in the univariate analysis were introduced as variables in the Cox model for multifactor analysis, and the results showed that MTV, D* and ADC were independent

Table 2 Summary of characteristics

Characteristics	Value
Age (years)	62.85 ± 9.63
Gender	
Male	29(47.54%)
Female	32(52.46%)
Pathological subtype	
Adenocarcinoma	46(75.41%)
Squamous carcinoma	15(24.59%)
Maximum diameter (mm)	27.39 ± 16.78
TNM staging	
I ~ II	24(39.34%)
III ~ IV	37(60.66%)
Operation	
yes	32(52.46%)
no	29(47.54%)
EGFR mutation	
yes	10(16.39%)
no	51(83.61%)
PFS(month)	17.00 (12.00, 21.75)
OS(month)	18.00 (14.75, 22.85)
PET/MRI-derived Parameters	
SUV _{max}	5.90(4.38, 10.40)
MTV(mL)	4.82(2.19, 7.91)
TLG(g)	14.32(4.56, 37.61)
ADC(x 10 ⁻³ mm ² /s)	1.42(1.27, 1.56)
D (x 10 ⁻³ mm ² /second)	1.20(1.02, 1.30)
f (%)	34.62(24.49, 69.75)
D*(x 10 ⁻⁵ mm ² /second)	49.68(16.59, 94.33)

PFS Progression-free survival, OS Overall survival, SUV_{max} Maximum standard uptake value, MTV Metabolic tumor volume, TLG Total lesion glycolysis, D Diffusion coefficient, f Perfusion fraction, D* Pseudo diffusion coefficient, ADC Apparent diffusion coefficient, EGFR Epidermal Growth Factor Receptor

Table 3 Prognostic analysis of OS

Parameters	univariate analysis		multifactor analysis	
	HR (95% CI)	P-value	HR (95% CI)	P-value
Gender	0.399 (0.133—1.197)	0.101	/	/
Age	1.037(0.975—1.102)	0.249	/	/
Diameter	0.046 (0.000—2820.388)	0.583	/	/
Pathological subtype	3.541 (1.239—10.118)	0.018	5.407 (0.794—36.837)	0.085
TNM staging	5.372 (1.178—24.491)	0.030	5.189 (0.336—80.143)	0.238
Operation	5.393 (1.483—19.610)	0.011	0.420(0.090—1.947)	0.267
EFGR mutation	0.846(0.189—3.785)	0.827	/	/
SUV _{max}	1.165 (1.026—1.324)	0.018	1.124 (0.844—1.497)	0.423
MTV	1.162 (1.082—1.248)	<0.001	1.216 (1.020—1.450)	0.029
TLG	1.036 (1.019—1.053)	<0.001	0.995 (0.943—1.050)	0.862
ADC	0.008 (0.000—0.123)	0.001	0 (0.000—0.010)	0.001
D	0.124(0.019—0.813)	0.003	2.060(0.003—1546.416)	0.831
f	1.001(0.999—1.004)	0.315	/	/
D*	0.980(0.963—0.998)	0.031	0.933(0.886—0.982)	0.008

All factors with $P < 0.05$ in univariate analyses were included in multivariate regression analyses. The bold typeface in the table indicates the logistic regression analyses with statistical significance

EFGR Epidermal growth factor receptor, SUV_{max} maximum standard uptake value, MTV Metabolic tumor volume, TLG Total lesion glycolysis, D Diffusion coefficient, f Perfusion fraction, D* Pseudo diffusion coefficient, ADC Apparent diffusion coefficient, HR Hazard ratio, CI Confidence interval

Table 4 Prognostic analysis of PFS

Parameters	univariate analysis		multifactor analysis	
	HR (95% CI)	P-value	HR (95% CI)	P-value
Gender	0.453 (0.152—1.353)	0.156	/	/
Age	1.034(0.974—1.099)	0.269	/	/
Diameter	0.045 (0.000—958.904)	0.543	/	/
Pathological subtype	3.286 (1.152—9.374)	0.026	3.348 (0.576—19.447)	0.178
TNM staging	4.600 (1.028—20.573)	0.046	1.910 (0.145—25.072)	0.622
Operation	5.105 (1.420—18.354)	0.013	0.747 (0.155—3.605)	0.717
EFGR mutation	0.908(0.203—4.059)	0.899	/	/
SUV _{max}	1.155 (1.019—1.309)	0.024	1.138 (0.842—1.537)	0.401
MTV	1.135 (1.063—1.213)	<0.001	1.189 (1.005—1.407)	0.043
TLG	1.033 (1.016—1.049)	<0.001	0.987 (0.936—1.042)	0.642
ADC	0.013 (0.001—0.179)	0.001	0 (0.000—0.012)	0.002
D	0.111(0.017—0.728)	0.022	0.685(0.002—277.791)	0.902
f	1.001(0.999—1.004)	0.351	/	/
D*	0.978(0.961—0.996)	0.018	0.931(0.887—0.978)	0.004

All factors with $P < 0.05$ in univariate analyses were included in multivariate regression analyses. The bold typeface in the table indicates the logistic regression analyses with statistical significance

EFGR Epidermal growth factor receptor, SUV_{max} Maximum standard uptake value, MTV Metabolic tumor volume, TLG Total lesion glycolysis, D Diffusion coefficient, f Perfusion fraction, D* Pseudo diffusion coefficient, ADC Apparent diffusion coefficient, HR Hazard ratio, CI Confidence interval

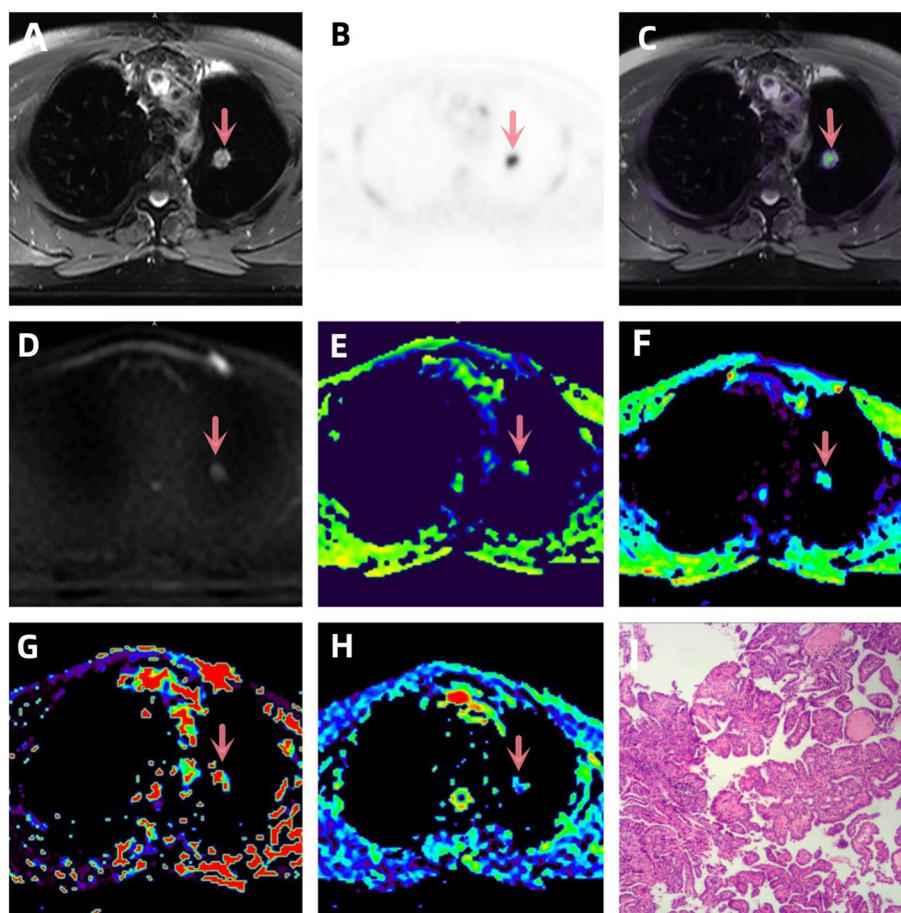


Fig. 1 A-I a patient with lung adenocarcinoma (arrowheads, stage IVB). **A** T2WI, **B** PET original image, $SUV_{max} = 7.72$, $MTV = 1.207$, $TLG = 6.033$, **C** PET and T2WI fusion map, **D** DWI original image ($b = 1000 \text{ s/mm}^2$), **E** ADC pseudo-color map, $ADC = 2.035 \times 10^{-3} \text{ mm}^2/\text{s}$, **F** D pseudo-color map, $D = 1.212 \times 10^{-3} \text{ mm}^2/\text{s}$, **G** D^* pseudo-color map, $D^* = 48.45 \times 10^{-5} \text{ mm}^2/\text{s}$, **H** f pseudo-color map, $f = 31.62 \times 10^{-3}\%$, **I** hematoxylin and eosin (H&E) staining image

predicting factors for OS and PFS in NSCLC patients (Tables 3, 4; Figs. 1, 2).

Discussion

Due to the high malignancy, aggressiveness and susceptibility to distant metastasis of NSCLC, the fatality rate increases year by year [22]. Accurate assessment of the prognosis of NSCLC patients can help to develop better treatment plans and improve the 5-year survival rate. Compared with PET/CT, PET/MR can reduce radiation dose, improve soft tissue contrast, and provide functional information of the lesion, which shows higher value in early prediction of lung cancer treatment effect [23–26].

SUV_{max} is the most commonly used semi-quantitative PET metabolic parameter in clinical practice. Some studies have explored its value in the prognostic assessment of NSCLC, but no unanimous conclusion has been reached. In the present study, OS and PFS were significantly lower in the $SUV_{max} > 5.90$ group than in the

$SUV_{max} \leq 5.90$ group, and SUV_{max} was an influential factor for OS and PFS in NSCLC patients. This is consistent with the findings of Liu et al. [27], however, Erdem et al. [28] and Nawara et al. [29] concluded that SUV_{max} did not play a role in the survival of NSCLC patients. These inconsistent results may be due to the fact that SUV_{max} is influenced by multiple factors, such as blood glucose, FDG injection scan time, device model, image reconstruction method, and partial volume effect. On the other hand, SUV_{max} is a single pixel value, unlike MTV and TLG which can combine multiple factors to reflect more comprehensively the volumetric load and overall metabolic situation of the tumor. MTV and TLG have already been considered as prognostic indicators for a variety of malignancies, such as esophageal cancer [30], laryngeal cancer [31] and nasopharyngeal cancer [32]. This study used univariate Cox regression analysis to show that higher MTV and TLG were significantly associated with worse OS ($P < 0.001$) and PFS ($P < 0.001$) in patients with

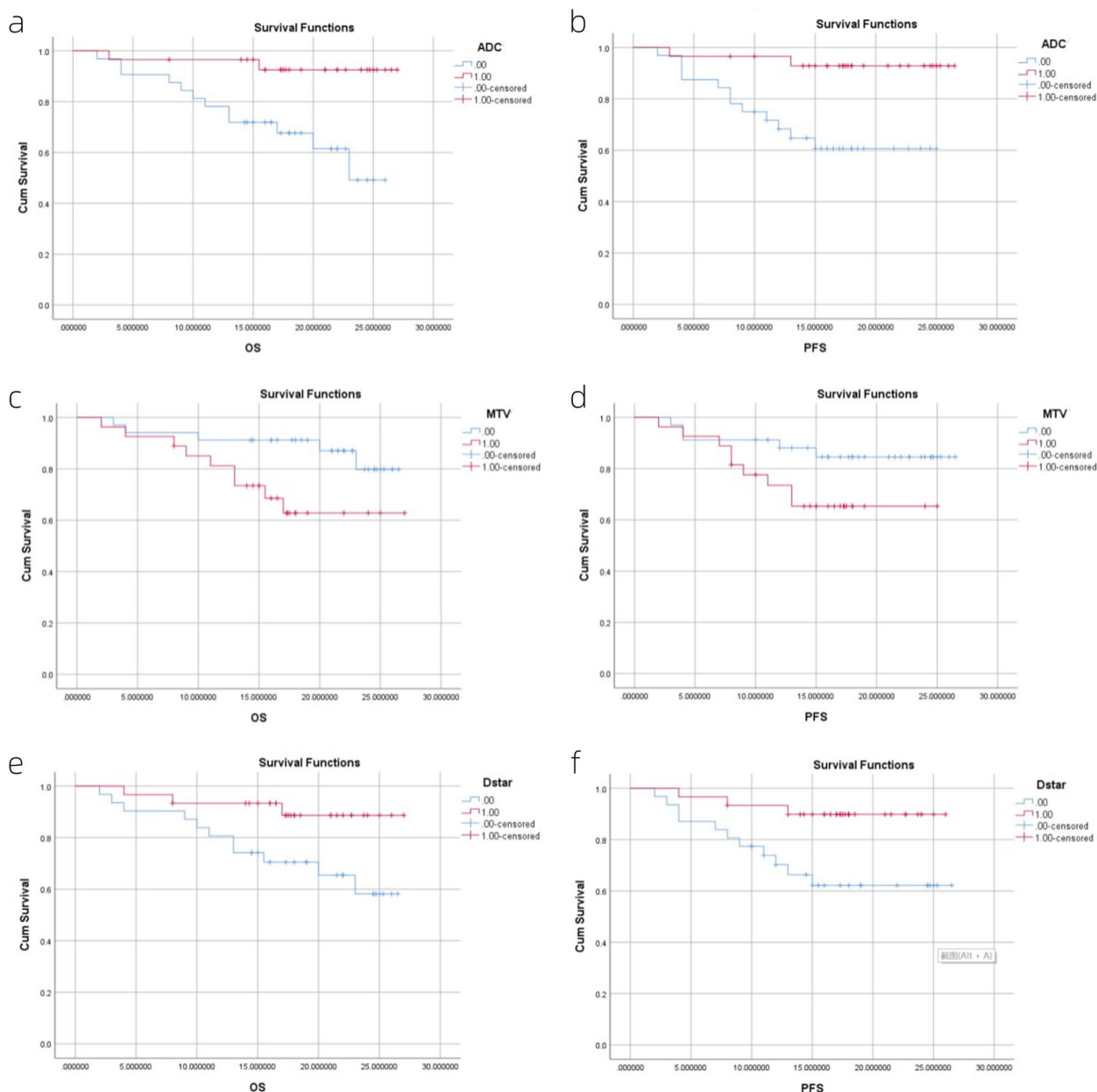


Fig. 2 Kaplan–Meier survival curves of progression-free survival and overall survival stratified by prediction model. **a** The *P*-value of log-rank is 0.004; **b** the *P*-value of log-rank is 0.005; **c** the *P*-value of log-rank is 0.035; **d** the *P*-value of log-rank is 0.085; **e** the *P*-value of log-rank is 0.032; **f** the *P*-value of log-rank is 0.014. 1 means greater than the median, 0 means less than the median

treated NSCLC, and MTV was also an independent predicting factor for PFS and OS in NSCLC patients. Salavati et al. [33] showed that pretreatment tumor volume parameters, including MTV and TLG, had a strong prognostic effect and similar discriminatory power on OS in patients with locally advanced NSCLC by assessing the relationship between each parameter and the outcome of 196 NSCLC patients using Cox regression analysis. The results of Wen et al. [34] also validated that stage I/II

NSCLC cases with increased MTV and TLG had a higher risk of side effects and that TLG was associated with an increased risk of death.

ADC is the representative parameter of DWI, which is usually influenced by cell density and can reflect the degree of restricted diffusion of water molecules in the tissue [35]. The parenchymal part of the tumor shows high signal on ADC, which can effectively highlight the lesion. Normally, the more obvious the diffusion

restriction of water molecules, the smaller the ADC value [36]. The multifactorial regression analysis in our study showed that ADC was an independent influence on OS and PFS in NSCLC patients. This is similar to the results of previous studies by Ohno et al. [19], in which ADC could be used as a functional indicator to assess the non-surgical outcome of NSCLC patients. This may be due to the fact that tumors with lower ADC values tend to have necrosis, hypoxia, acidification, and poor perfusion, resulting in lower therapeutic sensitivity to radiotherapy and chemotherapy, and therefore a poorer prognosis [37–39].

D is one of the IVIM parameters, which is influenced by cell density and the composition of extracellular matrix, and can reflect the diffusion of water molecules in tissue. This means that when the ratio of nuclei to the cytoplasm in tissues is high, or when the diffusion movement of water molecule is limited, resulting in a small extracellular space, the D value will be decreased [40]. In the IVIM sequence, both D^* and f are perfusion-related parameters, however, they represent different features of blood perfusion. D^* mainly reflects the average blood flow velocity, while f measures the fraction of blood volume in the capillary network, reflecting the microscopic translation movement related to blood microcirculation [41]. In this study, patients with high D^* value and D value group had higher OS than the low value group, and patients with high D^* value group had higher PFS than the low value group too. In addition, Cox regression analysis showed that D^* was also an independent influencing factor for OS and PFS. This is consistent with the study of Shi C [42] et al. This may be due to the rapid cell proliferation and micro-vascularity of tumor invasion resulting in decreased D^* values. In this study, there was no statistical difference between the high f -value group and the low f -value group. The reason for this result may be different treatment schemes will affect the f -value result. On the other hand, confounding factors, such as the properties of the tissue in the magnetic field, echo time, and relaxation time of the MRI scan, may also greatly affect the f -value [43]. Therefore, the potential of f in evaluating tumor microcirculation changes needs further study.

This study has several limitations. First, the relatively small number of NSCLC cases, due to the prospective nature of the study. It would lead to partial selection bias, and further studies with multiple centers and large samples are needed. Second, the ROIs of DWI and IVIM avoid necrosis, cystic degeneration and vascular areas, which may not be conducive to a comprehensive evaluation of tumor tissue structure. This is due to the large variation in these areas between lesions, which can interfere significantly with the parameter values.

Third, the effect of cardiac and macrovascular pulsations on parameter measurements was not considered in this study.

Conclusion

In summary, SUV_{max} , MTV, TLG, D , D^* and ADC derived from ^{18}F -FDG PET/MR imaging are all influential factors in the prognosis of NSCLC patients. Moreover, MTV, D^* and ADC are independent predicting factors for poor prognosis of NSCLC patients. These parameters can be jointly applied in clinical practice to predict treatment response and survival of NSCLC patients, and have important value in developing the personalized treatment and improving the survival for patients. In the future, the combination of PET/MR multi-models to predict NSCLC survival may be a new direction.

Abbreviations

PET/MR	Positron emission tomography-magnetic resonance
NSCLC	Non-Small cell lung cancer
SUV_{max}	Maximum standard uptake value
MTV	Metabolic tumor volume
TLG	Total lesion glycolysis
D	Diffusion coefficient
f	Perfusion fraction
D^*	Pseudo diffusion coefficient
ADC	Apparent diffusion coefficient
DWI	Diffusion-weighted imaging
IVIM	Intravoxel incoherent motion
HR	Hazard ratio
OS	Overall survival time
PFS	Progression-free survival time
OSME	Ordered subset maximum expectation iteration method
MRAC	MR-based attenuation correction
SUV_{mean}	Mean standardized uptake value
ICC	Intragroup correlation coefficient

Acknowledgements

We acknowledge all those who participated in this research. In addition, Han Jiang is grateful for the love received from Wensheng Zheng, I miss you, grandpa.

Authors' contributions

HJ: Data curation, Methodology, Formal analysis, Writing-Original draft preparation. ZL: Methodology, Writing-Reviewing and Editing. NM: Methodology, investigation. YL: Project administration, Investigation. PF: Project administration, Investigation. FF: Funding acquisition, investigation. YY: Project administration, Investigation. JY: Software, Writing-Reviewing and Editing. ZW: Software. All authors reviewed the manuscript. MW: Conceptualization, Funding acquisition, Methodology, Writing-Reviewing and Editing, Validation.

Funding

This work was supported by the Zhengzhou Collaborative Innovation Major Project [grant number 20XTZX05015]; the medical science and technology project of Henan Province [grant number SBGJ202101002]; the Henan provincial science and technology research projects [grant number 212102310689]; and the Henan Province Medical Science and technology public relations plan joint project [grant number LHGJ20210001]. The funding bodies played no role in the design of the study and collection, analysis, and interpretation of data and in writing the manuscript.

Data availability

The datasets used and/or analyzed during the current study available from the corresponding author on reasonable request.

Declarations

Ethics approval and consent to participate

This retrospective study was approved by the Ethics Committee of Henan Provincial People's Hospital (2021 Lungren Trial No.148), and the requirement for informed consent was obtained. All methods were carried out in accordance with relevant guidelines and regulations.

Consent for publication

Not applicable.

Competing interests

The authors declare no competing interests.

Author details

¹Department of Medical Imaging, Henan Provincial People's Hospital, Zhengzhou, Henan, China. ²Department of Magnetic Resonance, The First Affiliated Hospital of Xinxiang Medical University, Xinxiang, Henan, China. ³Zhengzhou University People's Hospital, Zhengzhou, Henan, China. ⁴Henan University People's Hospital, Zhengzhou, Henan, China. ⁵Beijing United Imaging Research Institute of Intelligent Imaging, United Imaging Healthcare Group, Beijing, China. ⁶Central Research Institute, United Imaging Healthcare Group, Shanghai, China.

Received: 27 June 2023 Accepted: 30 September 2024

Published online: 29 October 2024

References

- Torre LA, Bray F, Siegel RL, et al. Global cancer statistics, 2012. *CA Cancer J Clin.* 2015;65(2):87–108.
- Ettinger DS, Akerley W, Borghaei H, et al. Non-small cell lung cancer. *J Natl Compr Canc Netw.* 2012;10(10):1236–71.
- Im HJ, Pak K, Cheon GJ, et al. Prognostic value of volumetric parameters of ¹⁸F-FDG PET in non-small-cell lung cancer: a meta-analysis. *Eur J Nucl Med Mol Imaging.* 2015;42(2):241–51.
- Shi A, Wang J, Wang Y, Guo G, Fan C, Liu J. Predictive value of multiple metabolic and heterogeneity parameters of 18F-FDG PET/CT for EGFR mutations in non-small cell lung cancer. *Ann Nucl Med.* 2022;36(4):393–400. <https://doi.org/10.1007/s12149-022-01718-8>.
- Shao X, Niu R, Jiang Z, et al. Role of PET/CT in Management of Early Lung Adenocarcinoma. *AJR Am J Roentgenol.* 2020;214(2):437–45. <https://doi.org/10.2214/AJR.19.21585>.
- Tosi D, Pieropan S, Cattoni M, et al. Prognostic Value of 18F-FDG PET/CT Metabolic Parameters in Surgically Treated Stage I Lung Adenocarcinoma Patients. *Clin Nucl Med.* 2021;46(8):621–6. <https://doi.org/10.1097/RLU.0000000000003714>.
- Mirshahvalad SA, Metsger U, Basso Dias A, et al. 18F-FDG PET/MRI in Detection of Pulmonary Malignancies: A Systematic Review and Meta-Analysis. *Radiology.* 2023;307(2):e221598. <https://doi.org/10.1148/radiol.221598>.
- Moran A, Wang Y, Dyer BA, et al. Prognostic Value of Computed Tomography and/or 18F-Fluorodeoxyglucose Positron Emission Tomography Radiomics Features in Locally Advanced Non-small Cell Lung Cancer. *Clin Lung Cancer.* 2021;22(5):461–8.
- Xu Y, Hosny A, Zeleznik R, et al. Deep Learning Predicts Lung Cancer Treatment Response from Serial Medical Imaging. *Clin Cancer Res.* 2019;25(11):3266–75.
- Wu LM, Xu JR, Hua J, et al. Can diffusion-weighted imaging be used as a reliable sequence in the detection of malignant pulmonary nodules and masses? *Magn Reson Imaging.* 2013;31(2):235–46.
- Tondo F, Saponaro A, Stecco A, Lombardi M, Casadio C, Carriero A. Role of diffusion-weighted imaging in the differential diagnosis of benign and malignant lesions of the chest-mediastinum. *Radiol Med.* 2011;116(5):720–33.
- Le Bihan D, Breton E, Lallemand D, Aubin ML, Vignaud J, Laval-Jeantet M. Separation of diffusion and perfusion in intravoxel incoherent motion MR imaging. *Radiology.* 1988;168(2):497–505. <https://doi.org/10.1148/radiol.168.2.3393671>.
- Bergamino M, Nespodzany A, Baxter LC, et al. Preliminary Assessment of Intravoxel Incoherent Motion Diffusion-Weighted MRI (IVIM-DWI) Metrics in Alzheimer's Disease. *J Magn Reson Imaging.* 2020;52(6):1811–26. <https://doi.org/10.1002/jmri.27272>.
- Someya Y, Imai M, Imai H, et al. Investigation of breast cancer microstructure and microvasculature from time-dependent DWI and CEST in correlation with histological biomarkers. *Sci Rep.* 2022;12(1):6523. Published 2022 Apr 20. <https://doi.org/10.1038/s41598-022-10081-7>
- Gao S, Du S, Lu Z, et al. Multiparametric PET/MR (PET and MR-IVIM) for the evaluation of early treatment response and prediction of tumor recurrence in patients with locally advanced cervical cancer. *Eur Radiol.* 2020;30(2):1191–201. <https://doi.org/10.1007/s00330-019-06428-w>.
- Liu Y, Wang X, Cui Y, et al. Comparative Study of Monoexponential, Intravoxel Incoherent Motion, Kurtosis, and IVIM-Kurtosis Models for the Diagnosis and Aggressiveness Assessment of Prostate Cancer. *Front Oncol.* 2020;10:1763. Published 2020 Sep 11. <https://doi.org/10.3389/fonc.2020.01763>
- Fang T, Meng N, Feng P, et al. A Comparative Study of Amide Proton Transfer Weighted Imaging and Intravoxel Incoherent Motion MRI Techniques Versus (18) F-FDG PET to Distinguish Solitary Pulmonary Lesions and Their Subtypes. *J Magn Reson Imaging.* 2022;55(5):1376–90. <https://doi.org/10.1002/jmri.27977>.
- Li Z, Luo Y, Jiang H, et al. The value of diffusion kurtosis imaging, diffusion weighted imaging and 18F-FDG PET for differentiating benign and malignant solitary pulmonary lesions and predicting pathological grading. *Front Oncol.* 2022;12:873669. Published 2022 Jul 29. <https://doi.org/10.3389/fonc.2022.873669>
- Ohno Y, Koyama H, Yoshikawa T, et al. Diffusion-weighted MRI versus 18F-FDG PET/CT: performance as predictors of tumor treatment response and patient survival in patients with non-small cell lung cancer receiving chemoradiotherapy. *AJR Am J Roentgenol.* 2012;198(1):75–82.
- Ohno Y, Yui M, Yamamoto K, et al. Chemical Exchange Saturation Transfer MRI: Capability for Predicting Therapeutic Effect of Chemoradiotherapy on Non-Small Cell Lung Cancer Patients. *J Magn Reson Imaging.* 2023;58(1):174–86.
- Shieh G. Choosing the best index for the average score intraclass correlation coefficient. *Behav Res Methods.* 2016;48(3):994–1003.
- Abstracts of Presentations at the Association of Clinical Scientists 143rd Meeting Louisville, KY May 11–14, 2022. *Ann Clin Lab Sci.* 2022;52(3):511–525.
- Messerli M, de Galiza Barbosa F, Marcon M, et al. Value of PET/MRI for assessing tumor resectability in NSCLC—intra-individual comparison with PET/CT [published online ahead of print, 2018 Oct 11]. *Br J Radiol.* 2018;92(1093):20180379.
- Wehrli HF, Sauter AW, Judenhofer MS, et al. Combined PET/MR imaging—technology and applications. *Technol Cancer Res Treat.* 2010;9(1):5–20.
- Balyasnikova S, Löfgren J, de Nijs R, et al. PET/MR in oncology: an introduction with focus on MR and future perspectives for hybrid imaging. *Am J Nucl Med Mol Imaging.* 2012;2(4):458–74.
- Sauter AW, Wehrli HF, Kolb A, et al. Combined PET/MRI: one step further in multimodality imaging. *Trends Mol Med.* 2010;16(11):508–15.
- Liu J, Wu L, Liu Z, et al. ¹⁸F-RGD PET/CT and Systemic Inflammatory Biomarkers Predict Outcomes of Patients With Advanced NSCLC Receiving Combined Antiangiogenic Treatment. *Front Oncol.* 2021;11:671912. Published 2021 Jun 4.
- Erdem V, Selimoğlu Şen H, Kömek H, et al. Prognostic factors in non-small cell lung cancer patients and prognostic importance of PET/CT SUV max value. *Tuberk Toraks.* 2012;60(3):207–17.
- Nawara C, Rendl G, Wurstbauer K, et al. The impact of PET and PET/CT on treatment planning and prognosis of patients with NSCLC treated with radiation therapy. *Q J Nucl Med Mol Imaging.* 2012;56(2):191–201.
- Hyun SH, Choi JY, Shim YM, et al. Prognostic value of metabolic tumor volume measured by 18F-fluorodeoxyglucose positron emission tomography in patients with esophageal carcinoma. *Ann Surg Oncol.* 2010;17(1):115–22.
- Chung MK, Jeong HS, Park SG, et al. Metabolic tumor volume of [18F]-fluorodeoxyglucose positron emission tomography/computed tomography predicts short-term outcome to radiotherapy with or without chemotherapy in pharyngeal cancer. *Clin Cancer Res.* 2009;15(18):5861–8.

32. Xie P, Yue JB, Zhao HX, et al. Prognostic value of ^{18}F -FDG PET-CT metabolic index for nasopharyngeal carcinoma. *J Cancer Res Clin Oncol*. 2010;136(6):883–9.
33. Salavati A, Duan F, Snyder BS, et al. Optimal FDG PET/CT volumetric parameters for risk stratification in patients with locally advanced non-small cell lung cancer: results from the ACRIN 6668/RTOG 0235 trial. *Eur J Nucl Med Mol Imaging*. 2017;44(12):1969–83.
34. Wen W, Piao Y, Xu D, et al. Prognostic Value of MTV and TLG of ^{18}F -FDG PET in Patients with Stage I and II Non-Small-Cell Lung Cancer: a Meta-Analysis. *Contrast Media Mol Imaging*. 2021;2021:7528971.
35. le Bihan D. Apparent diffusion coefficient and beyond: what diffusion MR imaging can tell us about tissue structure. *Radiology*. 2013;268(2):318–22.
36. Shen G, Jia Z, Deng H. Apparent diffusion coefficient values of diffusion-weighted imaging for distinguishing focal pulmonary lesions and characterizing the subtype of lung cancer: a meta-analysis. *Eur Radiol*. 2016;26(2):556–66.
37. Koh DM, Collins DJ. Diffusion-weighted MRI in the body: applications and challenges in oncology[J]. *AJR Am J Roentgenol*. 2007;188(6):1622–35. <https://doi.org/10.2214/AJR.06.140>.
38. Usuda K, Funasaki A, Sekimura A, et al. FDG-PET/CT and diffusion-weighted imaging for resected lung cancer: correlation of maximum standardized uptake value and apparent diffusion coefficient value with prognostic factors. *Med Oncol*. 2018;35(5):66. Published 2018 Apr 9.
39. Huang YS, Chen JL, Chen JY, et al. Predicting tumor responses and patient survival in chemoradiotherapy-treated patients with non-small-cell lung cancer using dynamic contrast-enhanced integrated magnetic resonance-positron-emission tomography. *Vorhersage von Tumoransprechen und Patientenüberleben bei den mit Chemoradiotherapie behandelten Patienten mit nicht-kleinzelligem Lungenkrebs mittels dynamischer kontrastverstärkter integrierter Magnetresonanz-Positronenemissionstomographie*. *Strahlenther Onkol*. 2019;195(8):707–718.
40. Yuan Z, Niu XM, Liu XM, et al. Use of diffusion-weighted magnetic resonance imaging (DW-MRI) to predict early response to anti-tumor therapy in advanced non-small cell lung cancer (NSCLC): a comparison of intravoxel incoherent motion-derived parameters and apparent diffusion coefficient. *Transl Lung Cancer Res*. 2021;10(8):3671–81. <https://doi.org/10.21037/tlcr-21-610>.
41. Lee EY, Yu X, Chu MM, et al. Perfusion and diffusion characteristics of cervical cancer based on intravoxel incoherent motion MR imaging—a pilot study. *Eur Radiol*. 2014;24(7):1506–13. <https://doi.org/10.1007/s00330-014-3160-7>.
42. Shi C, Liu D, Xiao Z, et al. Monitoring Tumor Response to Antivascular Therapy Using Non-Contrast Intravoxel Incoherent Motion Diffusion-Weighted MRI. *Cancer Res*. 2017;77(13):3491–501. <https://doi.org/10.1158/0008-5472.CAN-16-2499>.
43. Wang LL, Lin J, Liu K, et al. Intravoxel incoherent motion diffusion-weighted MR imaging in differentiation of lung cancer from obstructive lung consolidation: comparison and correlation with pharmacokinetic analysis from dynamic contrast-enhanced MR imaging. *Eur Radiol*. 2014;24(8):1914–22. <https://doi.org/10.1007/s00330-014-3176-z>.

Publisher's Note

Springer Nature remains neutral with regard to jurisdictional claims in published maps and institutional affiliations.